The iron limitation mosaic in the California Current System: Factors governing Fe availability in the shelf/near-shelf region

C. P. Till, [1,2*] J. R. Solomon,[3] N. R. Cohen, [4] R. H. Lampe, [4] A. Marchetti, [4] T. H. Coale,[5] K. W. Bruland[2]

[1]Chemistry Department, Humboldt State University, Arcata, California
[2]Ocean Sciences Department, University of California Santa Cruz, Santa Cruz, California
[3]Environmental Sciences Department, Humboldt State University, Arcata, California
[4]Department of Marine Sciences, University of North Carolina at Chapel Hill, Chapel Hill, North Carolina
[5]Integrative Oceanography Division, Scripps Institution of Oceanography, University of California San Diego, La Jolla, California

Abstract

The California Current System is a productive eastern boundary region off the coasts of Washington, Oregon, and California. There is strong seasonality to the region, with high levels of rainfall and river input to the coastal ocean during the winter season, and coastal and Ekman upwelling during the spring and summer. Iron (Fe) input to the coastal ocean during the winter months can be stored in the continental shelf mud belts and then be delivered to the surface ocean by upwelling in the spring and summer. There have been a number of studies providing strong evidence of Fe-limitation of diatom growth occurring in regions of the California Current System off of California, and the occurrence of Fe-limitation has been linked with narrow continental shelf mud belt width and low river input. We provide evidence for potential Fe-limitation of diatoms off the southern coast of Oregon in July 2014, just off the shelf break near Cape Blanco in a region with moderate shelf width and river input. Since eastern boundary regions account for a disproportionally large amount of global primary production, this observation of potential Fe-limitation in an unexpected near-shore region of the California Current System has implications for global models of primary productivity. In order to re-evaluate the factors impacting Fe availability, we utilize satellite imagery to compare with historical datasets, and show that unexpected levels of Fe can often be explained by eddies, plumes of upwelled water moving offshore, or lack of recent upwelling.

The California Current System is an eastern boundary regime along the Washington, Oregon, and California coasts. Eastern boundary upwelling regimes are characterized by nutrient-rich, coastally upwelled water leading to high levels of productivity. Eastern boundary regimes account for a disproportionally large amount of global primary productivity (Carr 2002), and therefore are important places to study factors governing primary productivity.

There is a strong seasonality to the physical processes occurring in the California Current System that has been well-documented (Huyer 1983; Lynn and Simpson 1987; Strub et al. 1987): in the spring and summer, equatorward, alongshore winds prevail, leading to Ekman transport moving surface waters offshore. High degrees of coastal upwelling ensue; Checkley and Barth (2009) calculated upwelling velocities of 10–20 m per day over the shelf. Upwelled waters are cold, highly saline, and rich in macronutrients, which leads to the high productivity frequently observed in these regions.

Iron (Fe), however, is not consistently upwelled in plentiful supply along with the macronutrients. Iron is particle reactive and fairly insoluble, resulting in remineralized Fe being scavenged out of the water column rather than building up in concentration, as occurs with macronutrients (Bruland et al. 2014). Instead, one of the main Fe sources to eastern boundary regions is the continental shelf (Johnson et al. 1999; Bruland et al. 2001; Berelson et al. 2003; Elrod et al. 2004; Lohan and Bruland 2008). Waters within the benthic boundary layer over the shelf sediments can become enriched in Fe through resuspension and diffusive flux, and coastal upwelling can transport this shelf-sourced Fe to the surface along with the other macronutrients. However, this source term of Fe does not vary directly with the upwelling source of macronutrients. As a result, certain regions along the California Current System have been shown to exhibit Fe-limitation of diatom blooms (Hutchins and Bruland 1998; Hutchins et al. 1998;

*Correspondence: claire.till@humboldt.edu

Bruland et al. 2001; Firme et al. 2003; King and Barbeau 2007; Biller et al. 2013).

Shelf width is an important factor governing the potential for Fe-limitation of phytoplankton growth (Hutchins et al. 1998; Chase et al. 2007; Biller et al. 2013). While the upwelling conditions are in the spring and summer, winter rains and storms lead to high river runoff delivering Fe to the coastal ocean. Much of the riverine sediment input to the ocean sinks onto the continental shelf mud belts at depths of 50–90 m (Wheatcroft et al. 1997; Xu et al. 2002), but Fe-rich particles can be resuspended from the shelf and upwelled to the surface during the spring/summer upwelling season (Johnson et al. 1999). In regions where there is a wide shelf in the 50–90 m depth range, there is more area to retain the Fe-rich riverine sediment, and more contact between the upwelling water and the mud belt sediment, leading to greater Fe supplied from coastal upwelling. Furthermore, reduced Fe(II) in the shelf sediment can flux into the overlying water column and be upwelled to the surface ocean as well, which comprises another significant source of Fe (Berelson et al. 2003; Elrod et al. 2004). As a result of these processes, both river input and shelf width are linked to phytoplankton biomass in the California Current System (Chase et al. 2007).

Previous studies identifying Fe-limitation in the California Current System have focused on regions off the coast of California (Hutchins et al. 1998; Bruland et al. 2001; Firme et al. 2003; King and Barbeau 2007; Biller et al. 2013). Further north, Lohan and Bruland (2008) investigated wide-shelf regions off the coast of northern Oregon, and found elevated concentrations of Fe. In this work, we present data between these previously sampled locations, from a region of the California Current System off the coast of southern Oregon near Cape Blanco where we sampled in July 2014. This region experiences moderate river input (Chase et al. 2007), and our sampling region was just offshore of a moderately narrow shelf; based purely on shelf width and river runoff, this is an unlikely location for Fe-limitation. However, we provide evidence for potential Fe-limitation of coastal diatoms in this region of the California Current System as well.

Finding this evidence for potential Fe-limitation in a region with moderate shelf width and river input led us to go a step further and re-evaluate the factors that impact Fe availability along the California Current coastline. Certainly, Fe availability changes as upwelled water ages and moves offshore, and Fe is depleted disproportionally faster than the macronutrients through both preferential uptake and scavenging (Firme et al. 2003). The Fe concentration in eastern upwelling regimes has been shown to drop sharply moving offshore of the shelf break at about 200 m (Bruland et al. 2005; Kudela et al. 2006; Biller and Bruland 2013), so in addition to shelf width and river input, whether a sample is taken on or offshore of the shelf break is a key factor governing Fe availability. Furthermore, eddies can contribute to upwelling and can move plumes of recent coastally upwelled water offshore (e.g., Biller and Bruland 2013, 2014; Biller et al. 2013), leading to Fe-replete conditions offshore of the shelf break. Conversely, a parcel of water above a wide shelf with plenty of river input may be Fe-limited due to lack of recent upwelling, especially due to the converse seasonality of both processes (where intermittent river input can be very low in the summer months when upwelling is strong). Interplay between all these factors impacts the availability of Fe in eastern boundary regions.

In this work, in addition to providing evidence for the potential for Fe-limitation off the coast of southern Oregon, we investigate the cause of the Fe-availability observed in historical datasets using satellite imagery to evaluate eddies and upwelling events. We focus on samples that exhibited Fe-availability that was not easily explained by sample location: we selected samples that exhibited Fe-limitation despite being taken inland of the shelf break, and samples that exhibited Fe-replete conditions despite being taken offshore of the shelf break. In this manner, we discuss many of the factors that govern Fe-availability and the interplay between them.

Methods

Study site and sample collection

The IRNBRU cruise took place off the coasts of California and Oregon in July 2014 aboard the R/V *Melville*. The summer of 2014 was characterized by unusually low wind and coastal upwelling in the California Current system (Zaba and Rudnick 2016). During the later part of our cruise in late July 2014, the southern Oregon coastline was the most southern region of the California Current system exhibiting active upwelling. We report Fe and nitrate concentration data from two transects off the coast of Oregon near Cape Blanco. Figure 1 shows sampling locations overlaid on sea surface temperature for clear days during the cruise. Daily throughout the cruise, we monitored satellite data of surface altimetry and sea surface temperature, and adjusted the cruise plan in order to best capture the current features. We targeted our investigations to upwelling and potentially Fe-limited regions. Surface hydrographic data (temperature, salinity, and fluoresence) were monitored with the ship's flow-through underway data system. Nutrient samples were analyzed for nitrate + nitrite, phosphate, and silicic acid with a Lachat QuickChem 800 Flow Injection Analysis System and standard spectrophotometric methods (Parsons et al. 1984). Surface samples as well as vertical profile samples were taken and analyzed for dissolved Fe shipboard with a method adapted from Lohan et al. (2006) (discussed below).

Surface samples were obtained through a surface tow-fish system (Bruland et al. 2005). The fish was towed in the surface water alongside the ship, deployed from the end of a boom off the starboard side. Seawater was cleanly pumped through Teflon lines throughout the ship. Nutrient analyses were performed every 1.5 min on the water flowing out the terminus of the Teflon line. Surface Fe samples were obtained from a valve earlier in this line. Iron samples were filtered through a

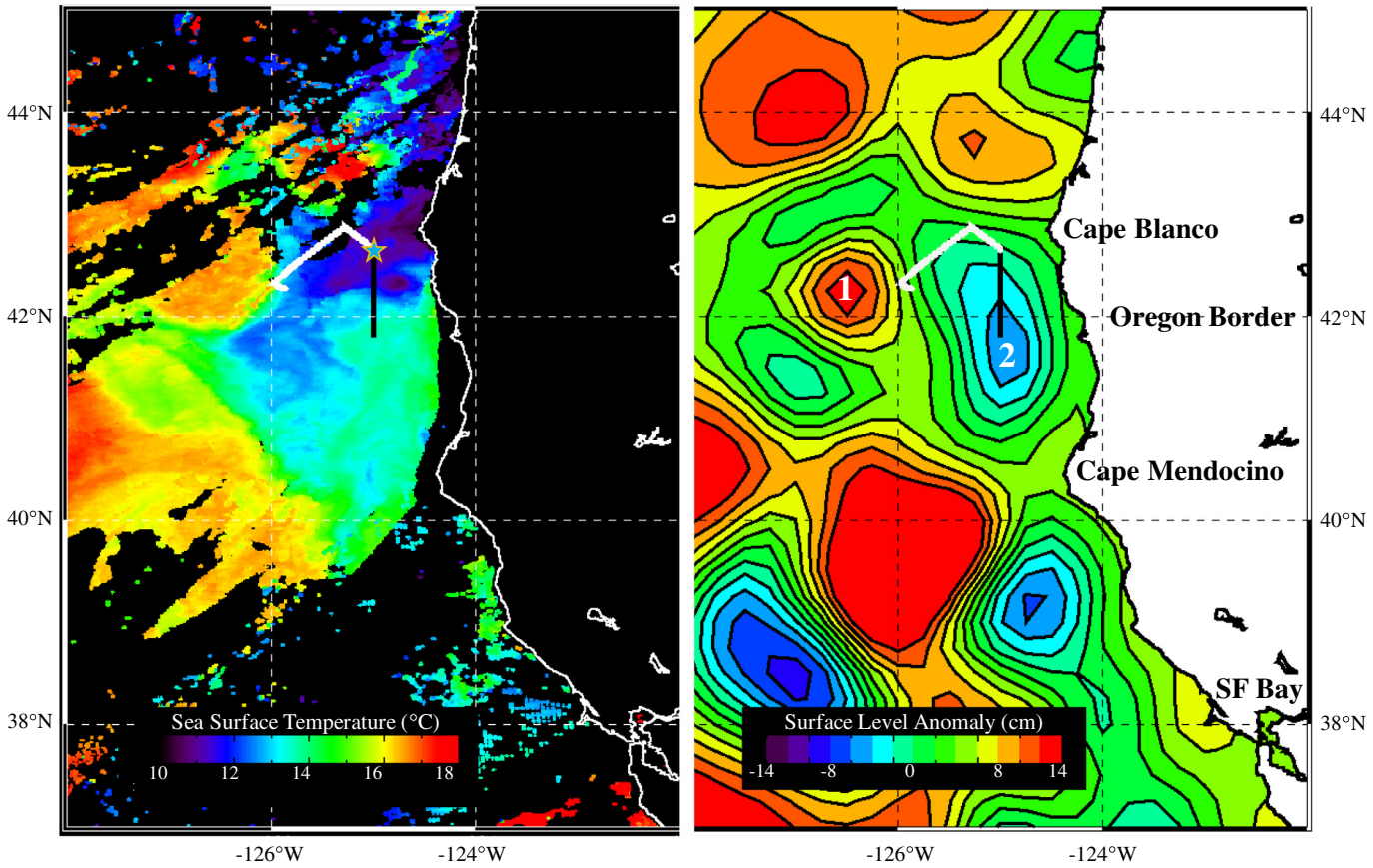

Fig. 1. Mean surface level anomaly and sea surface temperature on 20th July 2014, off the Oregon and Northern California coasts with the sampling site of the incubation experiment and the two transects we completed that day overlaid (incubation sampling site indicated by a star), transect 8, in black, and transect 9, in white). The anticyclonic and cyclonic eddies that are contributing to the movement of the upwelled plume of water offshore are labeled 1 and 2, respectively.

0.2 μm polysulfone membrane AcroPak-200® capsule filter into low-density polyethylene bottles that had been rigorously cleaned as in the GEOTRACES cookbook (Cutter et al. 2014). Sample bottles for Fe were stored in weak (pH ~ 2) trace metal grade HCl and rinsed three times with sample before filling. Iron samples were acidified to pH ~ 2 with quartz-distilled HCl and let sit for at least an hour before analysis.

Fe incubations and assessment of Fe status in diatoms

An incubation experiment was performed shipboard during our cruise using seawater as described by Marchetti et al. (2017). After completing transect 9, the ship steamed back to the intersection of the two transects and seawater was collected from the near surface (15 m) at 42.7°N, 125.0°W, a site of freshly upwelled coastal waters (Fig. 1). This seawater was distributed into acid-cleaned 10 L Cubitaners® (Hedwin Corporation) using trace metal clean techniques. For sample collection from initial conditions, triplicate cubitainers were filtered immediately. Others were incubated on deck at ~ 30% incident irradiance with control, Fe-enriched (5 nmol L^{-1} iron chloride), and Desferrioxamine b (DFB)-amended (200 nmol L^{-1}) treatments. DFB is an Fe-chelating ligand that reduces Fe availability to phytoplankton and is used to provide a treatment with induced Fe-limitation (Wells 1999; Marchetti and Maldonado 2016). Treatments were conducted in triplicate and sampled after 48 h and 72 h through destructive sampling.

Chlorophyll *a* (Chl *a*) measurements were obtained by gravity filtering of ~ 400 mL of seawater through a 5 μm polycarbonate filter followed by vacuum filtration through a GF/F filter using a series filter cascade for size fractionation. Filters were frozen at –80°C until analysis. Extractions were performed shipboard using 90% acetone kept at –20°C for 24 h followed by fluorometric quantification with a Turner Designs 10-AU fluorometer using the acidification method (Parsons et al. 1984). Size fractions were added together to yield total Chl *a*.

Maximum quantum yield (F_v/F_m) was measured by fast repetition rate fluorometry (FRRF) using Satlantic FIRe fluorescence-induction and relation system (Kolber et al. 1998; Gorbunov and Falkowski 2005). Samples were acclimated to low light for 20 min then a saturating pulse (20,000 μmol photons m^{-2} s^{-1}) of blue light was applied for a duration of 100–200 μs. The average of 50 iterations was obtained using a single-turnover flash. Data were blank-corrected using 0.2 μm filtered seawater.

In addition to monitoring changes through nutrient drawdown, phytoplankton biomass and F_v/F_m, the assessment of iron status in two ecologically dominant diatom genera, *Pseudo-nitzschia* and *Thalassiosira*, were determined via molecular approaches. Eukaryotic mRNA sequences from the incubations were assembled, annotated, and quantified as described in Cohen et al. (2017). The *Pseudo-nitzschia* Iron Limitation Index (Ps-n ILI) was quantified as described by Marchetti et al. (2017) such that a positive ratio indicates iron stress or limitation. The iron status of *Thalassiosira* was examined through differences in gene expression of the iron-sensitive genes, flavodoxin (*FLDA*) and iron starvation induced protein 3 (*ISIP3*) (Chappell et al. 2015). Gene expression values were normalized and significance was assessed with DESeq2 using Benjamini and Hochberg adjusted *p*-values ≤ 0.05 (Benjamini and Hochberg 1995; Love et al. 2014).

Shipboard dissolved Fe analysis method

Iron analysis was preformed shipboard to give us near-real-time data, allowing us to better select our sampling sites. Dissolved iron concentrations were determined through preconcentrating the Fe on a chelating resin before adding the colorimetric agent N,N-dimethyl-p-phenylenediaminedihydrochloride (DPD), and detecting the catalytically enhanced signal with a UV–vis spectrophotometer as outlined in Lohan et al. (2006). The seawater is loaded onto the resin at pH 2 because the Fe(III) that had been chelated with organic compounds is dissociated at pH 2 and is available to chelate with the resin. Additionally, loading at a low pH is advantageous when working with high concentrations of Fe that are insoluble at higher pHs. Lohan et al. (2006) used the NTA-type superflow resin, but due to lower blanks and better consistency, we followed the modification of Biller et al. (2013) and used Toyopearl Chelate-650 instead. Since Fe(II) is not recovered at pH 2 on this resin, whereas Fe(III) is recovered at > 93% (Biller et al. 2013), 10 μmol/L H_2O_2 is added to the sample before loading, which is sufficient to quantitatively oxidize reduced Fe (Lohan et al. 2005).

Satellite data for IRNBRU sampling and interpretation

In order to sample in the best possible locations based on current conditions, during the cruise we monitored satellite data daily for surface altimetry and temperature. The availability of temperature data was inconsistent due to frequent interference by clouds, but altimetry data was reliably available. Temperature data from the NOAA POES AVHRR satellite was downloaded from the NOAA coastwatch website (http://coastwatch.pfeg.noaa.gov/coastwatch/CWBrowser.jsp). Altimetry data was produced (including merging data from multiple satellites) and distributed by Aviso (http://www.aviso.altimetry.fr/). We imaged the satellite data with Interactive Data Language®, a product of Exelis Visual Information Solutions, a subsidiary of Harris Corporation (Exelis VIS).

Approach to historical sample comparison

Historical samples selected for analysis were sampled between the years 1996 and 2011 (Hutchins and Bruland 1998; Hutchins et al. 1998; Firme et al. 2003; King and Barbeau 2007; Biller et al. 2013; Biller and Bruland 2014). We defined a simple way to consider data "expected," which we would not consider further, and "unexpected," which we would investigate through the use of satellite data: Fe-replete conditions in samples taken over the shelf and Fe-limited conditions in samples taken offshore of the shelf break were considered expected, and the opposite sets of conditions were considered unexpected. Notably, we accepted these authors' conclusions about which samples were Fe-limited or Fe-replete and did not reassess any of their original datasets. Some used nutrient ratios and estimated growth rates (Biller et al. 2013; Biller and Bruland 2014) and some used incubation experiments (Hutchins and Bruland 1998; Hutchins et al. 1998; Firme et al. 2003; King and Barbeau 2007).

For each selected historical sampling date and location, both temperature and altimetry datasets were downloaded from NOAA coastwatch. The sea surface temperature data was captured over 3- or 8-d intervals, centered on the sampling date, to reduce cloud interference. Altimetry satellite data was averaged over a 1-month interval. Sea surface temperature and altimetry datasets for each historical sampling date and location were projected into ArcGIS® to produce figures that provide insights into the upwelling conditions during the time of sampling.

Historical sample locations selected for analysis were organized in an excel spreadsheet by latitude and longitude coordinates and uploaded into ArcGIS® as X – Y data. Sea surface temperature and altimetry for each historical sampling date and location was downloaded as an HDF file and projected into ArcGIS®. Bathymetry data, acquired from the NOAA Geophysical Data Center, was downloaded as a shapefile. Latitude and longitude data was retrieved from ESRI, a supplier of geographic information software, and downloaded as a ready shapefile.

Results and discussion

Overview of transects

Two transects were sampled off the southern Oregon coast (Fig. 1). Transect 9 (the east/west transect) immediately followed the completion of transect 8 (the north/south transect). As noted by the ~ 10°C water at the surface, there was some upwelling occurring at the time we sampled (Fig. 1). The geostrophic flow of the anticyclonic and cyclonic eddies was moving that recently upwelled water offshore and to the southwest, in a plume traveling between the two eddies (Fig. 1; eddies labeled 1 and 2, respectively).

On the northern end of transect 8, there is clear evidence of upwelling with the low temperatures (~ 9.9–10.6°C) and high salinities (33.3–33.7) (Fig. 2). The lowest temperature and highest salinity occur at about 42.3°N, and there is a corresponding increase in the nitrate and silicic acid concentrations at this latitude. Despite the active upwelling inferred from the low

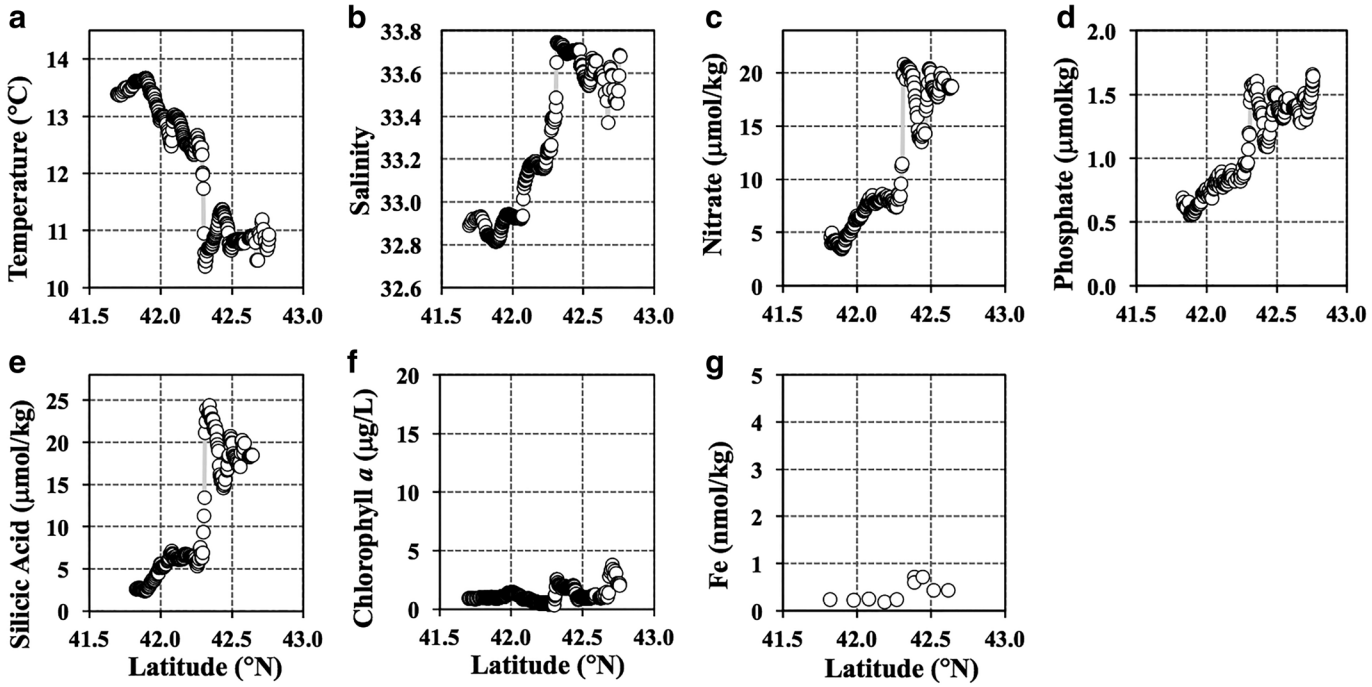

Fig. 2. (**a**) Temperature, (**b**) salinity, (**c**) nitrate, (**d**) phosphate, (**e**) silicic acid, (**f**) Chl *a* fluorescence, and (**g**) dissolved Fe vs. latitude along transect 8. The scale of the Fe distribution extends to 5 nmol/kg in order to emphasize that all these Fe concentrations are low relative to the maximum concentrations measured in this region. In other upwelling regions during this cruise, Fe concentrations up to 3 nmol/kg were measured (Till, unpubl.).

temperature and high salinity values, and the resulting high concentrations of nitrate, phosphate, and silicic acid (21 μmol/kg, 1.6 μmol/kg, and 24 μmol/kg, respectively), the fluorescence is relatively low (2.5–3.3 μg/L). Dissolved Fe has a maximum concentration of 0.7 nmol/kg, which occurs at 42.4°N; at this same location there is a slight decrease in the nitrate and silicic acid concentrations and a slight increase in the temperature, but the salinity is still high. This could be indicative of a plume of slightly older upwelled water that has had time to warm and have the nutrients be slightly drawn down.

Transect 9 exhibits similar characteristics to transect 8 (Fig. 3). There are low temperatures (10.1–10.6°C) and high salinities (33.4–33.7) in the eastern part of the transect, corresponding with high nitrate (17–21 μmol/kg), phosphate (1.3–1.6 μmol/kg) and silicic acid (18–23 μmol/kg), indicative of upwelling. Meanwhile the fluorescence remains relatively low (1.1–3.8 μg/L), as does the dissolved Fe concentration (0.35–0.4 nmol/kg), in the upwelling zone. At 125.3°W, the salinity and nutrients dropped markedly as the transect moved out of the upwelled water and into lower salinity water influenced by the California Current. As a result, we altered course and headed southwest back into the high salinity and nutrient rich upwelled waters. At the western end of the transect, there was a marked salinity drop and rise in temperature as the transect left the upwelling filament and began to enter the anticyclonic eddy (labeled "1" on Fig. 1b).

Due to the range of upwelling signatures across the two transects, we divide the region into zones (Fig. 4). The strongest upwelling signal is the plume identifiable by its high salinity, which we crossed twice (zone 1). We define the borders of the upwelling zone to be when salinity transitions to 33.4, both times we crossed the upwelling plume. That leaves a region north of the plume with lower salinity (zone 2), the western part of transect 9 (zone 3), and the southern part of transect 8 (zone 4).

Plotting these measured attributes (temperature, nitrate, phosphate, silicic acid, fluorescence, and dissolved Fe) against salinity should reveal the extent to which their distributions are governed by upwelling (Fig. 5). Temperature and macronutrients exhibit robust correlations with salinity, suggesting a strong influence of upwelling on these parameters. Fluorescence shows no trend with salinity, nor does Fe except at the highest salinity values, which indicates that there is an upwelling source of Fe in this region. The northern peak of transect 9 exhibits the most distinct characteristics of all the zones: for a given salinity, it has higher macronutrient concentrations and lower temperatures than the other parts of the study site, and yet does not have correspondingly higher fluorescence. The western region of transect 9 and the southern region of transect 8 are remarkably similar in salinity space, with the exception of fluorescence, which is higher along transect 9.

Investigation of potential Fe-limitation of diatoms

Evidence for Fe-limitation was derived from Fe-amendment and removal incubation experiments, nutrient ratios and estimations of in situ growth rates. Incubation experiments rely on

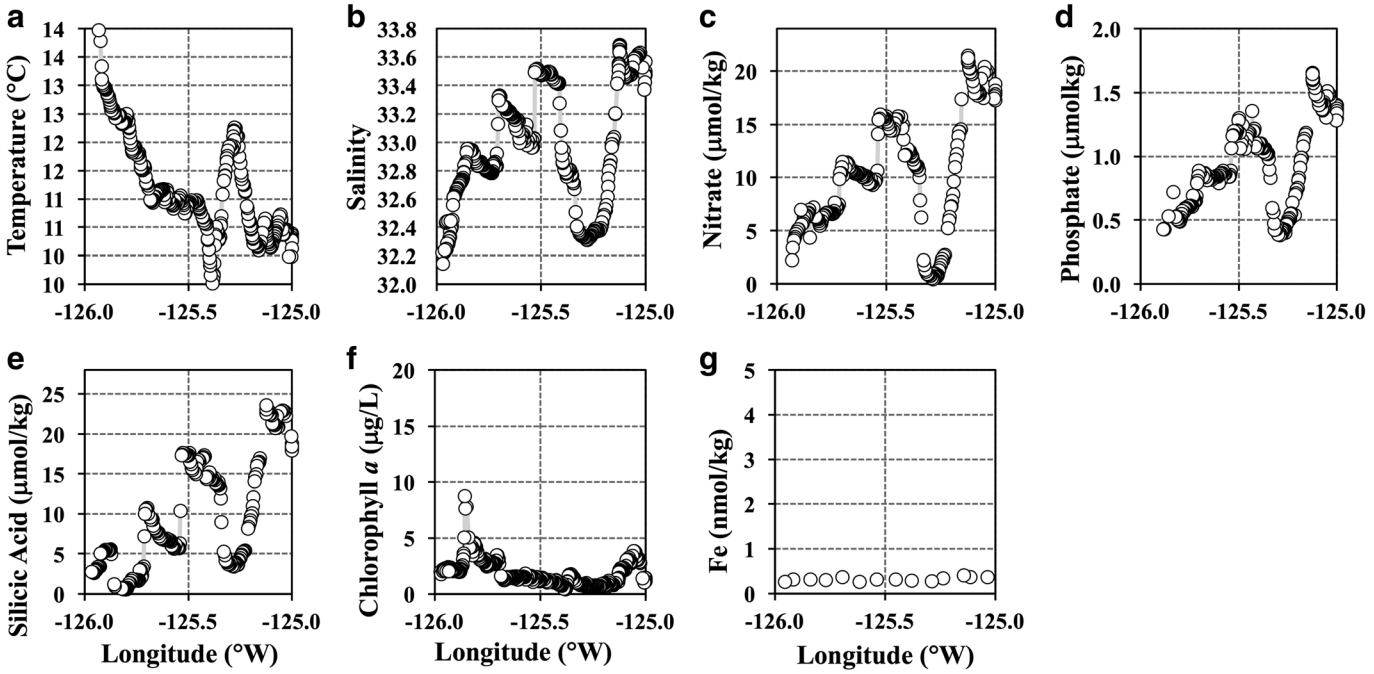

Fig. 3. (**a**) Temperature, (**b**) salinity, (**c**) nitrate, (**d**) phosphate, (**e**) silicic acid, (**f**) Chl *a* fluorescence, and (**g**) dissolved Fe vs. longitude along transect 9. The scale of the Fe distribution was chosen for the reasons mentioned in Fig. 2.

increases in biomass that are significantly different from the unamended control in order to measure the *potential* for Fe-limitation to occur. Furthermore, although estimates of growth rates and Fe requirements may be used to comment on Fe status (see below), these physiological parameters can vary considerably depending on the diverse phytoplankton taxa present (Marchetti and Maldonado 2016), and therefore can only support the potential for Fe-limitation to occur in regions of the coastal California Current System. In this study, we provide insight into the Fe nutritional status of diatom assemblages through the use of molecular indicators, which compliment traditional incubation data and can be used to distinguish between growth-induced Fe-limitation within incubations and Fe-limitation of the ambient diatom community.

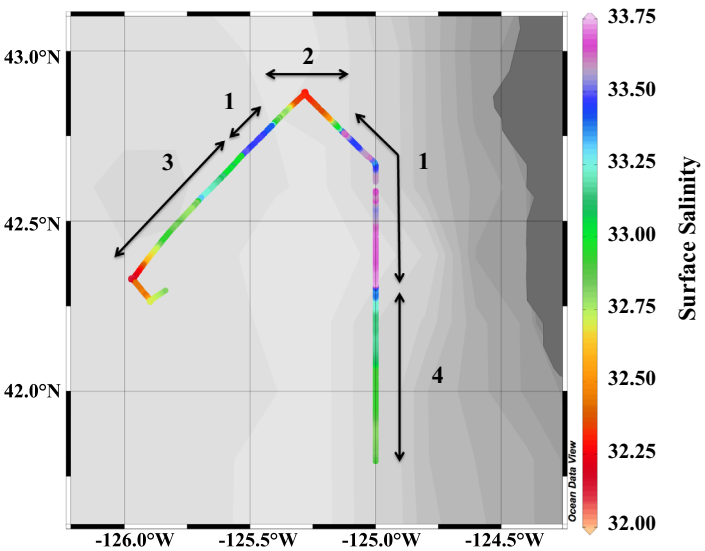

Fig. 4. Surface salinity along both transects. Note that cooler colors (purple, blue) correspond with higher salinities. The upwelling plume (zone 1), identifiable by its high salinity, was crossed twice. North of the upwelling plume there is a decrease in salinity (zone 2). The remaining western part of transect 9 and southern part of transect 8 are zones 3 and 4, respectively.

To assess the potential for Fe-limitation in these water conditions, a shipboard incubation was performed just after transect 9 in the freshly upwelled waters of zone 1 (42.7°N, 125.0°W, Fig. 1). The results of this incubation are plotted in Fig. 6. Figure 6a,b show nitrate drawdown and Chl *a* measured at an initial time point and 48 and 72 h following incubation in an unamended control, after Fe enrichment (+Fe) and after iron chelator addition (+DFB) used to induce Fe-limitation. Following 48 h, the +Fe treatment exhibited lower nitrate concentrations and higher chlorophyll concentrations than the control and +DFB treatments, indicating a difference in the phytoplankton biomass accumulation rates. After 72 h, significant differences in these parameters were observed comparing the +Fe treatment relative to the control but not in the +DFB treatment relative to the control (ANOVA, $p < 0.05$). Remaining nitrate concentrations were 7.27 ± 0.35 μmol L^{-1} in the control, 9.81 ± 3.76 μmol L^{-1} in the +DFB treatment and nearly depleted in the +Fe treatment. Correspondingly, total chlorophyll concentrations reached 4.3 ± 0.7 μg L^{-1} in the control, 4.16 ± 0.78 μg L^{-1} in the +DFB treatment and

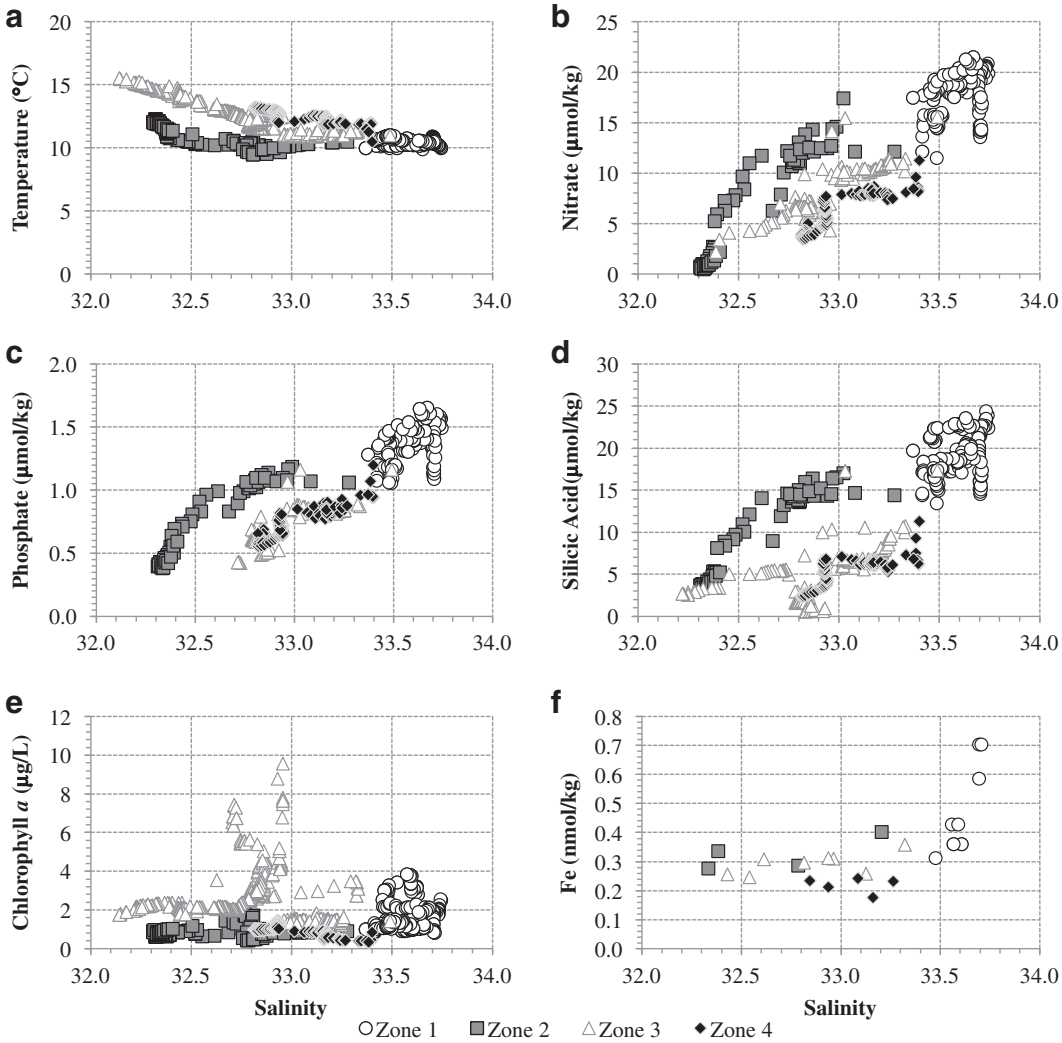

Fig. 5. Temperature (**a**), nitrate (**b**), phosphate (**c**), silicic acid (**d**), fluorescence (**e**), and dissolved Fe (**f**) vs. salinity for both transect 8 and transect 9. The transects are split into zones based on salinity transitions across 33.4: Southern T8: transect 8 south of the major salinity transition at 33.4; upwelling T8 and T9: the upwelling region that we crossed twice defined by major salinity transitions at 33.4; Western T9: transect 9 west of the major salinity transition at 33.4; Northern Peak T9: the northern most part of T9, north of the upwelling zone.

12.4 ± 1.0 μg L^{-1} in the +Fe treatment. Notably, these differences in nutrient drawdown and phytoplankton accumulation rates provide strong evidence for Fe-limitation after 72 h in the control treatment. Consistent with these trends, the F_v/F_m values in the control and +DFB treatment decreased within 48 h when compared to the initial time point and the +Fe treatment, further supporting the induction of Fe-limitation in the control and +DFB treatment (Fig. 6c).

In our incubation experiments, members of the diatom genera *Pseudo-nitzschia* and *Thalassiosira* were among the most dominant based on relative transcript abundance (Cohen et al. 2017). Marchetti et al. (2017) developed a *Pseudo-nitzschia* Iron-Limitation Index (Ps-n ILI), which is plotted for this incubation experiment in Fig. 6d. Positive values are indicative of probable iron stress/limitation of *Pseudo-nitzschia*. In the +DFB treatment, the Ps-n ILI became positive following 48 h following incubation, confirming the onset of induced Fe-limitation of *Pseudo-nitzschia* in this treatment. In the control and +Fe treatment, values remained negative following 48 h of incubation, yet notably the Ps-n ILI becomes less negative in the control after 48 h compared with the initial time point and the +Fe treatment (Fig. 6c). This suggests that *Pseudo-nitzschia* cells in the non-amended community were moving toward—but had not yet reached—absolute Fe-limitation after 48 h. Similarly, elevated transcript abundances of *FLDA* and *ISIP3* in *Thalassiosira* in the control were observed (Fig. 6e). In particular, *ISIP3* expression was similar to that of the DFB treatment suggesting the onset of Fe-stress. These trends are consistent with those observed by Chappell et al. (2015) that demonstrated Fe stress in *Thalassiosira oceanica* in offshore waters close to our region of study using a similar molecular approach.

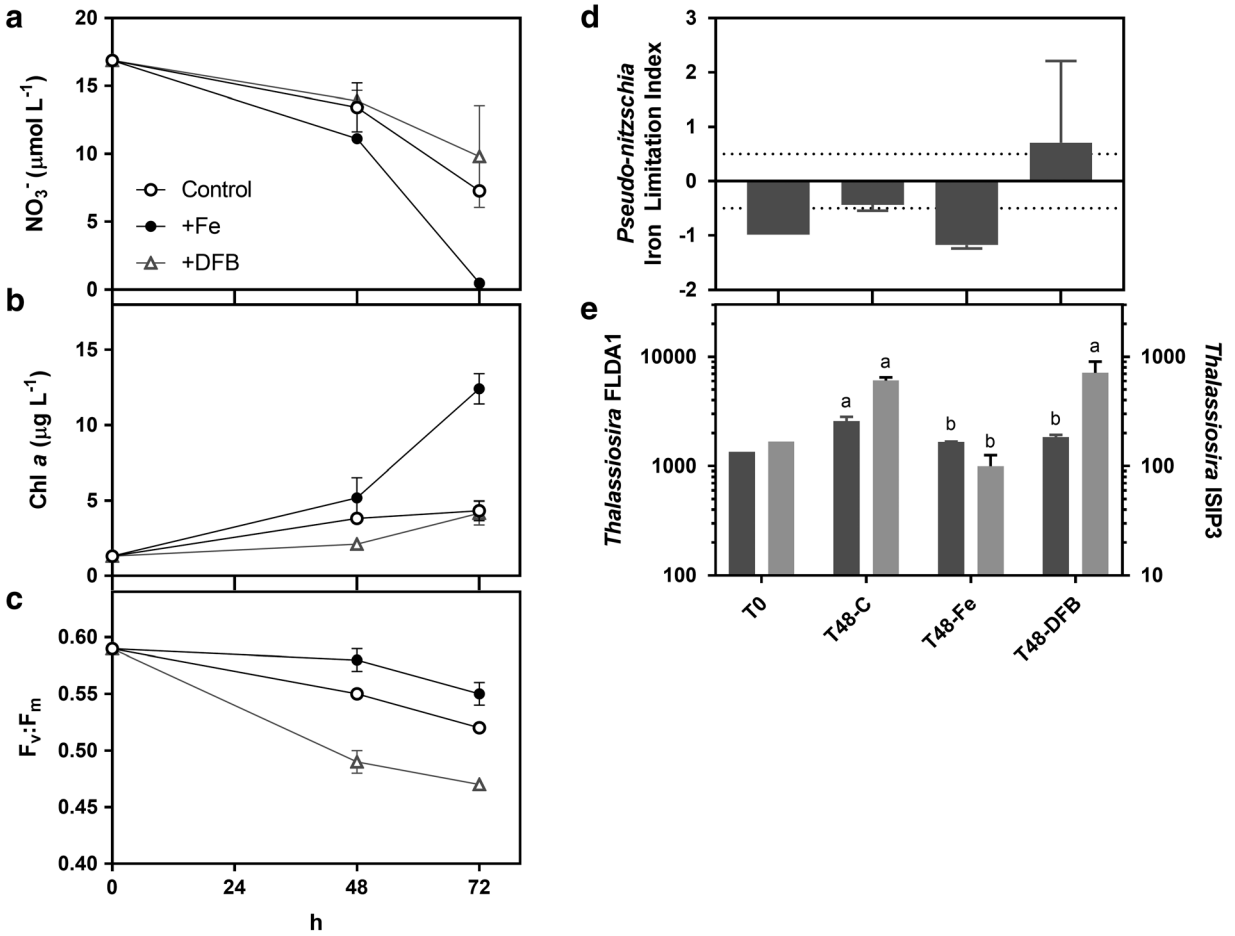

Fig. 6. Measurements from the incubation experiment. (**a–c**) Nitrate, chlorophyll, and $F_v : F_m$ from the initial conditions, 48 h, and 72 h after incubation for the control (open circle), Fe (closed circle), and DFB (open triangle) treatments. (**d**) The *Pseudo-nitzschia* Iron Limitation Index values for the incubations at 0 h and 48 h. Values within dashed lines indicate the potential for iron stress. Values below that range indicate iron-replete growth whereas values above that range indicate iron limitation. (**e**) *Thalassiosira* flavodoxin (dark gray) and ISIP3 (light gray) normalized counts. Higher comparative expression indicates increased iron stress. Letters denote significant differences across treatments for each gene as determined with DESeq2 using Benjamini and Hochberg adjusted p-values ($p \leq 0.05$), with "a" indicating treatments that are significantly different from "b" treatments.

Taken together, the incubation experiment suggests that although diatoms in these freshly upwelled waters were likely not Fe-limited initially, induction of Fe-stress and subsequent limitation of diatom growth rates in the unamended controls as well as the +DFB treatment rapidly ensued due to the Fe demands needed to support the high rates of phytoplankton biomass accumulation. As a result, appreciable differences in phytoplankton biomass between the +Fe treatments and the unamended controls were observed following 72 h of incubation.

In order to investigate whether this potential for Fe-limitation was representative of the surrounding region as well as the incubation sampling site, we used nutrient and Fe concentration data with simply modeled estimates of growth rates and uptake ratios to assess the Fe-limitation potential along transects 8 and 9. The low Fe concentrations, high nitrate concentrations, and relatively low fluorescence in the upwelling regions of these transects indicate that the potential for Fe-limitation of diatoms as the upwelled water ages and Fe is drawn down is likely.

Biller et al. (2013) utilized two methods for investigating the extent of Fe-limitation in the California Current System by approaching the limitation from the perspectives of growth rate and biomass accumulation. Growth rates for specific types of phytoplankton can be calculated based on availability and half saturation constants of a limiting nutrient with the following well-established equation (Monod 1942):

$$\mu = \frac{\mu_{\max}[S]}{[S] + K_\mu} \tag{1}$$

where μ is the specific growth rate (under the conditions specified), $\mu_{\max}$ is the maximum growth rate under optimal conditions, $[S]$ is the ambient concentration of the nutrient, and K_μ is the half-saturation constant for the nutrient (where $\mu = 0.5\mu_{\max}$). Sarthou et al. (2005) compiled and reported values of $\mu_{\max}$ and K_μ for diatoms. As in Biller et al. (2013), we choose to estimate diatom growth rate using the average values reported by Sarthou et al. (2005): $\mu_{\max}$ = 1.5 d^{-1}, K_μ for Fe = 0.35 nmol L^{-1}, K_μ for

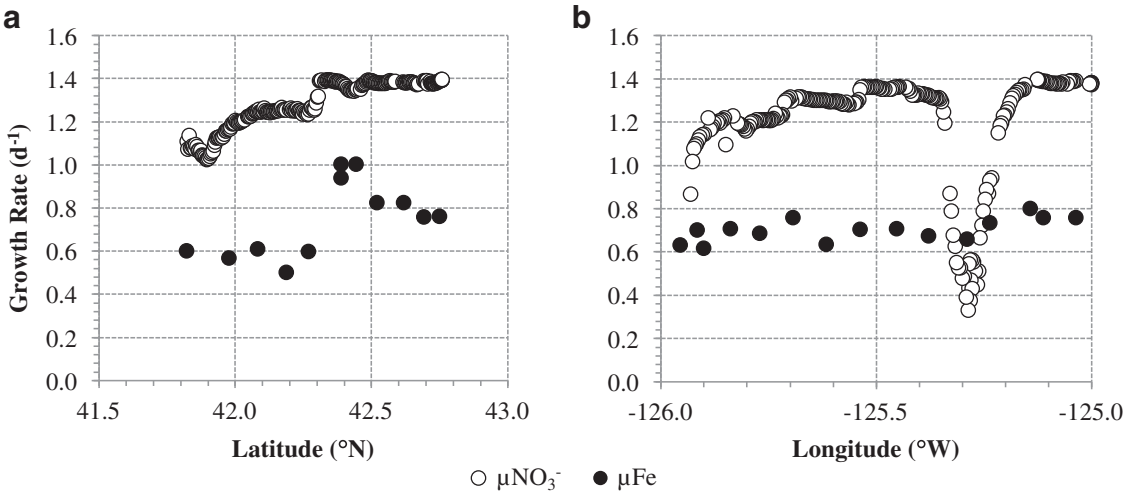

Fig. 7. Estimated growth rate calculated from Fe (μ_{Fe}) and nitrate (μ_{NO3-}) concentrations on (**a**) transect 8 and (**b**) transect 9. Note the different measurements on the *x*-axes. A μ_{Fe} lower than the μ_{NO3-} suggests that Fe is limiting diatom growth rate in that location.

N = 1.6 μmol L^{-1}. In a given time and place, the nutrient with the smallest specific growth rate is considered the growth-rate limiting nutrient. In the California Current System, nitrate and Fe are the two nutrients likely to be limiting in surface waters: when the specific growth rate calculated based on Fe concentrations (μ_{Fe}) is less than that based on the nitrate concentrations (μ_{NO3-}), then Fe is the growth-rate limiting nutrient. It is noteworthy that growth rates and K_μ values for Fe can vary extensively (Marchetti and Maldonado 2016), so it is crude to use averages as we do here. Again, we choose to do this as a back-of-the-envelope calculation to investigate whether the conditions observed in the incubation likely persist across the wider spatial area of our transects.

As mentioned previously, any locations where μ_{Fe} is lower than μ_{NO3-} suggest Fe-limitation of the growth rate of coastal diatoms. There is one region (~ 125.3°W, zone 2 in Fig. 4) where the nitrate concentrations are less than 2 μmol/kg and the μ_{NO3-} is less than the μ_{Fe} (Fig. 7). Apart from that location, the entirety of both transects show evidence of low enough Fe concentrations, relative to the elevated nitrate concentrations, that could limit the growth rate of coastal diatoms as well as their ability to accumulate biomass (Fig. 7).

An important caveat to this line of thought is that the current dissolved nutrient concentrations do not take into account prior Fe availability and uptake. For example, the ambient dissolved Fe may be low precisely *because* diatoms have recently taken up significant amounts, and therefore momentarily have sufficient Fe for high growth rates despite low ambient Fe levels. The measured dissolved Fe is that which was not yet taken up and was leftover. With these considerations firmly in mind, estimated growth rates can be used to provide an indication of Fe-availability, and are perhaps best used in conjunction with other metrics of physiology.

The other way that Biller et al. (2013) used to estimate Fe-limitation is by considering biomass accumulation. Coastal diatoms grow at near-optimal rates at 30 μmol mol^{-1} Fe to carbon (Bruland et al. 2001; Sunda and Huntsman 1995). Using the Redfield ratio for carbon to nitrogen (Redfield 1958), Biller et al. (2013) calculate a required Fe to nitrate ratio of 0.2 nmol/μmol. Therefore, if the ambient Fe to nitrate ratio is less than 0.2 nmol μmol^{-1}, coastal diatoms could be limited in their biomass accumulation by Fe rather than nitrate.

As with our growth rates and $K_{\mu,}$ estimations earlier, this is a coarse estimate of a value that can vary dramatically (Marchetti and Maldonado 2016). Again, we use these rough estimations to investigate whether it is likely that the conditions observed in the incubation are representative of the surrounding waters as well.

Along both transects, at all locations where nitrate was greater than 4 μmol/kg and both Fe and nitrate were measured, the Fe to nitrate ratio is well below 0.2 nmol/μmol Fe to nitrate (Fig. 8a,b). It is notable that even if calculated using a lower Fe to carbon ratio of 10 μmol mol^{-1}, which gives a threshold Fe to nitrate ratio of 0.07 nmol μmol^{-1}, there are many locations along both transects below that threshold. These low ratios indicate that Fe is likely the Liebig limiting nutrient for coastal diatoms at these locations.

Furthermore, low silicic acid to nitrate ratios has been connected with Fe-stress (Brzezinski et al. 2015). The usual upwelled ratio of silicic acid to nitrate along the California coast is 1.2 μmol/μmol (Zentara and Kamykowski 1977; Brzezinski et al. 2015), and throughout significant portions of both of these transects, the silicic acid to nitrate ratio is below the usual upwelled ratio of 1.2 μmol/μmol (Fig. 8c,d), which could likely have developed due to a relative lack of Fe in the phytoplankton community.

An important distinction between these two methods of assessing Fe-limitation of diatoms is that the growth rate calculation indicates which nutrient will limit growth rate under the *current* conditions, whereas nutrient ratios indicate which

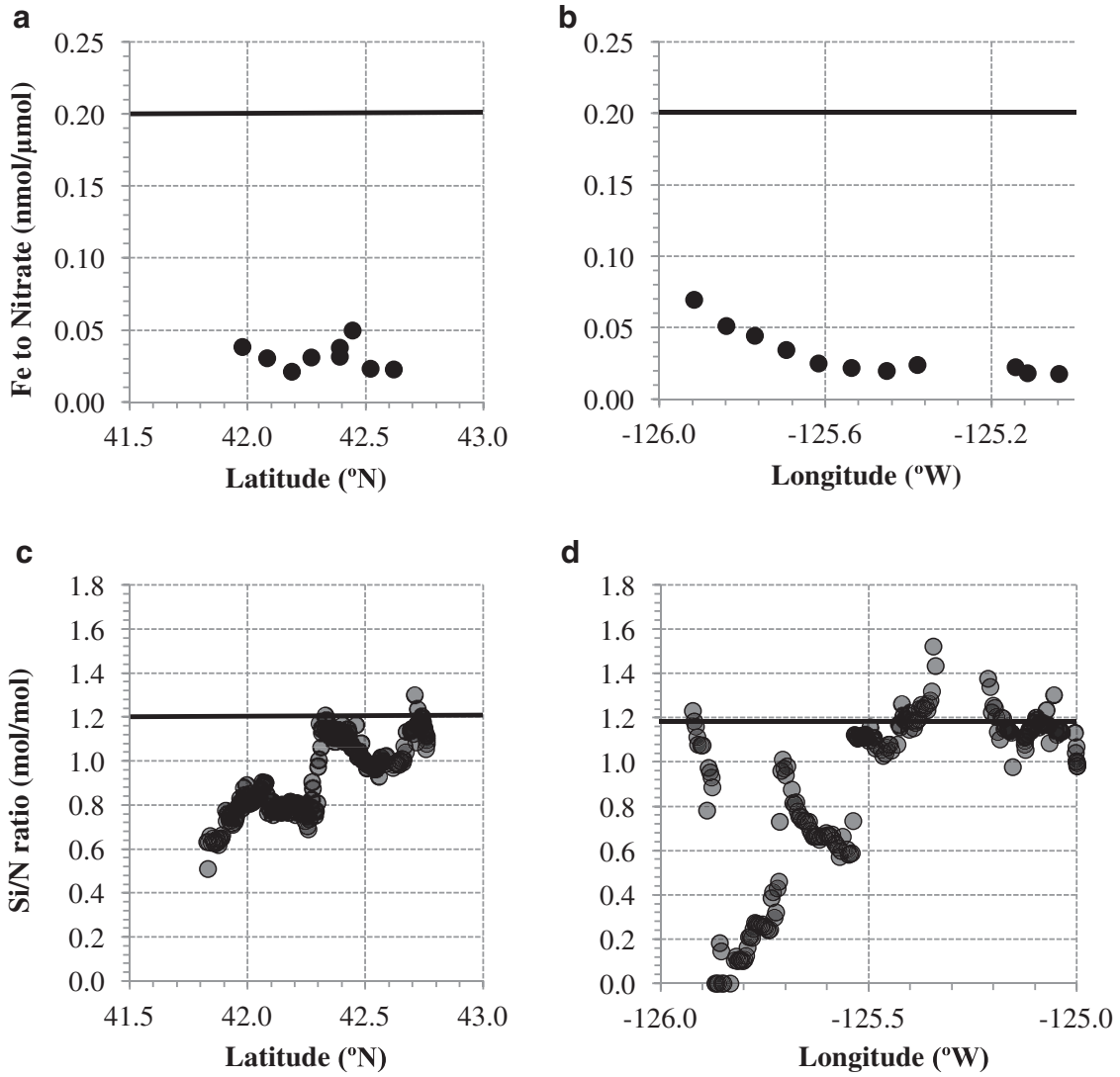

Fig. 8. Iron to nitrate ratio for transect 8 (**a**) and transect 9 (**b**) and silicic acid to nitrate ratio for transects 8 (**c**) and 9 (**d**) where nitrate concentrations are greater than 3.5 μmol/kg. Note the different measurements on the *x*-axes. Due to the number of data points in (c) and (d), each is plotted as a transparent grey circle; the regions with many overlapping data points appear black. An iron to nitrate ratio below 0.2 nmol/μmol (solid black line) suggests Liebig limitation of coastal diatoms, and a silicic acid to nitrate concentration below 1.2 μmol/μmol (solid black line) suggests deviation from the upwelled ratio through Fe-stress.

nutrient will become limiting first, as phytoplankton biomass accumulates and both macronutrients and Fe are drawn down. Both suggest the potential for Fe-limitation of diatoms along these transects.

Overall, we have assessed the potential for Fe-limitation of phytoplankton in this region off the coast of southern Oregon from many angles, targeting ecologically dominant diatoms and looking at overall Chl *a* production, nitrate drawdown and photosynthetic efficiency in an incubation experiment as well as using estimated growth rates and optimal nutrient ratios along the two transects. All evidence suggests the potential for Fe-limitation, particularly as freshly upwelled waters begin to age and biological activity and scavenging drive down the upwelled Fe. Although Fe-limitation has been well-studied in the California Current System off the coast of California, to the authors' knowledge this is the first reported occurrence to support possible Fe-limitation off the coast of Oregon, indicating that the range of the Fe-limitation mosaic should be extended slightly further north than was previously known. Additionally, and more importantly, this is identification of potential Fe-limitation in a region with moderate shelf width (Fig. 9) and river input (Chase et al. 2007), and therefore a region that traditionally would not be expected to feature Fe-limitation.

Fe-limitation in this new region of the California Current System

Since Fe-limitation in the California Current System has been often connected with narrow shelf width (Hutchins

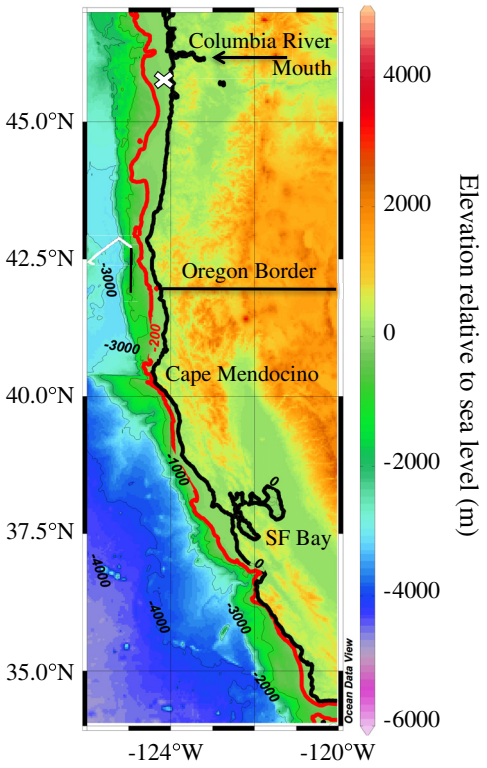

Fig. 9. Shelf width along the northern California and Oregon coastline, indicated by the distance between the 0 m and 200 m isobath. The cruise tracks for this work are overlaid in black (transect 8) and white (transect 9). Lohan and Bruland (2008)'s Oregon shelf sampling location is marked by the white cross. [Color figure can be viewed at wileyonlinelibrary.com]

et al. 1998; Chase et al. 2007; Biller et al. 2013), it is at first surprising that the region in which we observe evidence of potential Fe-limitation has a moderate shelf width and river input. However, the sampling locations were offshore of the shelf break (Fig. 9), and as noted previously, Bruland et al. (2005) and Kudela et al. (2006) have observed the dissolved Fe concentration rapidly decrease moving off the shelf break in eastern boundary regions (the Peru upwelling system and the coast of California, respectively). It is likely that a similar decrease in the surface Fe concentration occurs off this shelf break along the Oregon coastline. When Lohan and Bruland (2008) found elevated Fe in the shelf waters off the northern coast of Oregon, they sampled at a wider shelf region inland of the shelf break (Fig. 9). Lohan and Bruland (2008) were also very close to the Columbia River mouth (Fig. 9), which is a large source of Fe to the shelf in that region (Chase et al. 2007; Bruland et al. 2008). Since there is a moderate shelf width and river input off the southern coast of Oregon, it is possible that over the shelf itself there is sufficient supply of Fe from upwelling to avoid initial Fe-limitation, however as the upwelled water ages and advects offshore and biological activity occurs, Fe-limiting conditions could develop. Since eastern boundary regions account for a relatively high proportion of global primary productivity for their area (Carr 2002), finding evidence for potential Fe-limitation in this unexpected region of the California Current System has implications for global models of primary productivity.

Investigation of historical datasets

The possibility of Fe-limitation in a region with moderate shelf-width and moderate river flux region led us to investigate previously published historical data. We reviewed sampling datasets from previously published documents (Hutchins and Bruland 1998; Hutchins et al. 1998; Firme et al. 2003; King and Barbeau 2007; Biller et al. 2013; Biller and Bruland 2014) and selected samples to compare with historical satellite data. We specifically selected what we consider to be unexpected Fe availability: samples that the original authors determined to be Fe-limited despite being over the shelf break, and samples that they determined to be Fe-replete despite being offshore of the shelf break. From these historical data sets, 17 samples fit our criteria and were therefore flagged for further analysis, none of which were from Hutchins and Bruland (1998), King and Barbeau (2007) or Biller and Bruland (2014). Notably, there were only two cases of unexpected Fe-replete conditions, both from Firme et al. (2003), so this historical dataset exploration is by no means a thorough study of Fe-replete conditions offshore of the shelf break. Potentially the relative lack of unexpected Fe-replete conditions could indicate that they are less frequent than unexpected Fe-limited conditions.

Four samples from Firme et al. (2003) just south of Point Arena fit the selection criteria. Two of them were collected between 03 June 1999 and 17 June 1999 at 38.20° N, 123.20° W and 38.02° N, 123.25° W (Fig. 10a,b). These samples were taken over the continental shelf within the 200 m isobath but had Fe-limited conditions as determined by an Fe addition incubation (Firme et al. 2003). Figure 10a displays a relatively high temperature at the sampling region, suggestive of a relaxation period and therefore a lull in the supply of Fe from the shelf. Contrarily, the altimetry displays an average negative sea level anomaly (MSLA) at the point of sampling, suggesting upwelling (Fig. 10b). We attribute the contrasting signals to the fact that the altimetry data was averaged over a 1-month interval: since the SST does not indicate recent upwelling, and yet the altimetry of the month of June 1999 suggests upwelling, we infer that the sampling occurred just before an upwelling period that would then persist over the majority of the month June.

The other two samples from Firme et al. (2003) that fit our selection criteria were collected between 23 June 1999 and 11 July 1999, in a similar location: 38.45°N, 123.60° W and 37.75°N, 123.97°W, off the continental shelf beyond the 200 m isobath (Fig. 10c,d). Despite being offshore of the shelf break, these two samples had Fe-replete conditions as determined in Firme et al. (2003) by Fe addition incubation. We did verify with the data tables in Firme et al. (2003) that these samples had sufficient nitrate (13 and 21 μM) that it was not a

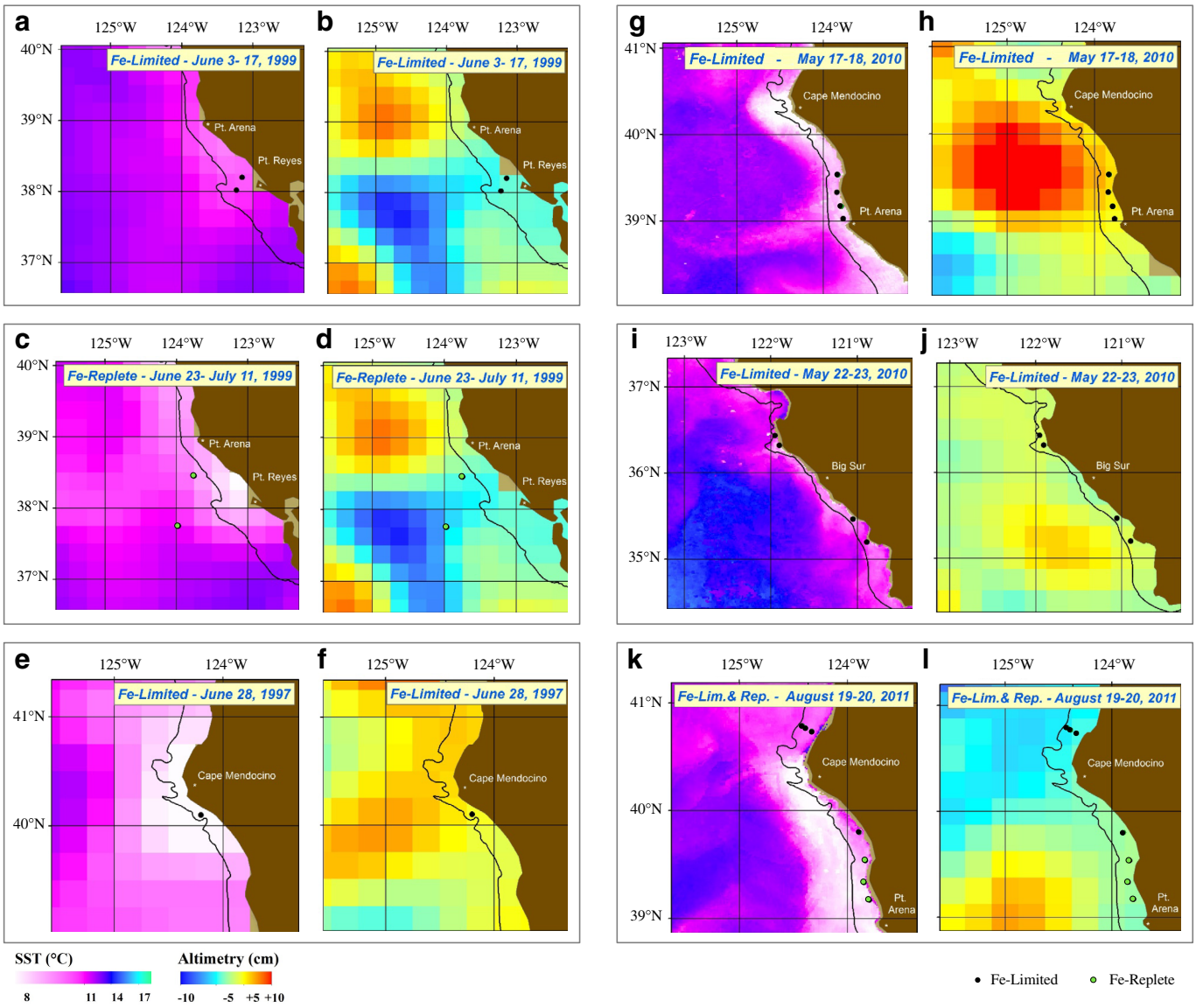

Fig. 10. Satellite data corresponding with historical samples selected from the datasets of Firme et al. (2003) (**a**–**d**), Hutchins et al. (1998) (**e**, **f**), and Biller et al. (2013) (**g**–**l**). Sample locations plotted in this figure correspond with all the samples from those papers that had unexpected Fe availability, which we define as Fe-replete samples from off the shelf break and Fe-limited samples from over the shelf. Some additional samples with expected levels of Fe availability are included as well for comparison. The 200 m isobaths is plotted on all panels in black. The left panel in each box displays sampling locations overlaid with satellite sea surface temperature data from the time of sampling (1-d averages at the beginning of the sampling time for the samples before 2000; 8-d averages centered on the middle of the sampling dates for the samples taken after 2000) with cooler colors representing cooler temperatures and warmer colors representing warmer temperatures. The right panel in each box displays the sampling locations overlaid with satellite altimetry data (mean sea level anomaly; monthly averages centered on the 16th of each month), with reds representing sea surface highs (downwelling conditions) and blues sea surface lows (upwelling conditions). The unusual Fe availability of these samples can be explained with the satellite data.

false Fe-replete signal due to nitrate limitation. Figure 10c displays cool recently upwelled water nearshore, much cooler than the previous month in the same location (Fig. 10a). This recently upwelled water is likely moving offshore passing close to the sampling region and is potentially replenishing the sampling locations with Fe. Figure 10d displays a dynamic upwelling and downwelling system in the sampling region, with the two sampling locations at the edge of an upwelling eddy. With the month-long averages for altimetry data centered on the 16th of each month, this altimetry distribution is the same as for the samples in Fig. 10b. However these offshore sampling locations are both closer to the upwelling eddy and were sampled during the greater degree of coastal upwelling, which could explain their greater degree of Fe availability.

One sample from Hutchins et al. (1998) fit within our selection criteria. It was located off the coast of Cape Mendocino at 40.10°N, 124.2°W on the shelf within the 200 m isobath, and

was collected on 28 June 1997 (Fig. 10e,f). The sample had Fe-limited conditions determined by an incubation experiment (Hutchins et al. 1998), despite being located on the shelf. It is also worth noting that Hutchins et al. (1998) classified it as a previously unrecognized type of Fe-limitation, where the addition of Fe altered the planktonic community composition, rather than the macronutrient utilization and particular organic carbon production. The historical satellite data of the sampling region (Fig. 10e,f) display relatively cold temperatures and a slightly positive altimetry at the point of sampling. Because of the low resolution of the satellite data from that long ago, it is difficult to tell whether the cooler temperatures plotted near the sample location actually overlapped with the sampling location, or whether there could have been smaller-scale features as are indicated in the more recent temperature datasets (Fig. 10g,i,k). Based on the positive altimetry value, we suggest that during sampling this region was experiencing a downwelling event, which explains why Hutchins et al. (1998) found this sample Fe-limited even though it was from inland of the shelf break.

The final historical samples investigated were retrieved from Biller et al. (2013). These datasets illustrate California's Fe-limitation mosaic among three different sampling dates and regions. During the first sampling interval, 17 May 2010–18 May 2010, four samples were collected North of Point Arena and South of Cape Mendocino (39.3338°N, 123.8410°W; 39.5358°N, 123.8305°W; 39.1718°N, 123.7918°W; 39.0303°N, 123.7690°W; Fig. 10g,h). The samples were collected on the continental shelf within the 200 m isobath and nevertheless had Fe-limited conditions determined by nutrient ratio analysis and growth rate calculations. However, the altimetry data indicates a large, strong anticyclonic eddy with about a +10 cm MSLA nearing the sampling region (Fig. 10h). We conclude that the upwelling was not strong or recent enough to lead to Fe-replete conditions, in part due to the presence of this eddy.

On 22 May 2010–23 May 2010, four samples collected on the continental shelf of Big Sur within the 200 m isobath had Fe-limited conditions as determined by nutrient ratio analysis and growth rate calculations (Biller et al. 2013). At the point of sampling, the SST data (Fig. 10i) displays an average temperature of ~ 9–11°C, and the altimetry data (Fig. 10j) displays an average of 0 cm. The moderate temperatures and minimal MSLA indicate that this location was sampled during minimal upwelling. Furthermore, the predominantly narrow shelf in this region does not supply much Fe even when upwelling does occur. Both of these factors likely led to the Fe-limited conditions observed.

Last, on 19 August 2011–20 August 2011, seven samples were collected along the continental shelf from just north of Cape Mendocino to Point Arena, within the 200 m isobath (Biller et al. 2013; Fig. 10k,l). The samples' Fe condition was determined by nutrient ratio analysis and growth rate calculations (Biller et al. 2013). These samples displayed an Fe-limitation mosaic, with the samples north of Cape Mendocino exhibiting Fe-replete conditions, and three of the four samples south of Cape Mendocino exhibiting Fe-limited conditions (Fig. 10k,l, green data points represent Fe-limited conditions and black points Fe-replete). The altimetry historical satellite data (Fig. 10l) was captured over a 1-month interval and shows general evidence of upwelling occurring, in particular off the coast of Cape Mendocino. With the high-resolution SST satellite data captured over a 3-d interval (Fig. 10k), it can be seen that there was cool upwelled water in the region of the black sample points only: there is a pocket of higher temperatures near shore just south of Cape Mendocino, where likely the winds had not been sufficiently alongshore to cause upwelling, and the one Fe-limited data point south of Cape Mendocino is in that region. The other data points south of the Cape are substantially in the heart of the coldest water indicative of the most recent upwelling (Fig. 10k), and correspondingly they were found to be Fe-replete. In contrast, the three Fe-replete samples north of Cape Mendocino were in warmer water indicative of a relaxation period, and correspondingly were found to have Fe-limited conditions. Through the use of high-resolution SST data, fine-scale features in the upwelling conditions can be observed, and in this case those features can explain the Fe-limitation mosaic observed.

Conclusions

We find evidence of potential Fe-limitation of coastal diatoms off the southern Oregon coast, in a region with moderate shelf width and river input. Several methods of evaluating potential Fe-limitation were used to investigate this: a shipboard incubation Fe-addition experiment was performed, which indicated that the incubated phytoplankton community quickly became Fe-limited after the first 48 h. In order to investigate whether this potential for Fe-limitation was more widespread than just the location of the incubation sampling site, surface transect data was used both to estimate growth rates of coastal diatoms and to calculate Fe to nitrate ratios to determine the Liebig limiting nutrient on biomass accumulation of coastal diatoms. Both of these methods also indicate that coastal diatoms should be limited by Fe in many locations of the two transects we analyzed. In comparison with previous work over the wide-shelf of the northern coast of Oregon that showed elevated Fe (Lohan and Bruland 2008), this work is further from the Columbia River mouth and just offshore of the shelf break rather than over the shelf. Identifying evidence of potential Fe-limitation off the southern Oregon coast in a region that, solely based on river input and shelf width, would be expected to be Fe replete during upwelling conditions indicates that near-shore Fe-limitation within the California Current System could be a more widely spread phenomena than was previously known, and has implications for models of global primary productivity.

Furthermore, since this new region of possible Fe-limitation has moderate shelf width and river input, we investigated the factors influencing Fe availability using historical Fe-limitation

datasets and satellite SST and MSLA data. The satellite data proved to be a powerful tool in identifying variations in upwelling conditions temporally and spatially in order to explain otherwise surprising measurements of Fe availability. From this investigation, we highlight that in addition to shelf width and river runoff, other factors including whether samples were taken on or offshore of the shelf break, plumes of upwelled water being advected offshore by eddies, fine-scale features in the upwelling conditions caused by geography or eddies, and variable upwelling conditions over time can all have a large impact on Fe availability in these dynamic regions.

References

Benjamini, Y., and Y. Hochberg. 1995. Controlling the false discovery rate: A practical and powerful approach to multiple testing. J. R. Stat. Soc. Ser. B Methodol. **57**: 289–300. doi:10.2307/2346101

Berelson, W., and others. 2003. A time series of benthic flux measurements from Monterey Bay, CA. Cont. Shelf Res. **23**: 457–481. doi:10.1016/S0278-4343(03)00009-8

Biller, D. V., and K. W. Bruland. 2013. Sources and distributions of Mn, Fe, Co, Ni, Cu, Zn, and Cd relative to macronutrients along the Central California coast during the spring and summer upwelling season. Mar. Chem. **155**: 50–70. doi:10.1016/j.marchem.2013.06.003

Biller, D. V., T. H. Coale, R. C. Till, G. J. Smith, and K. W. Bruland. 2013. Coastal iron and nitrate distributions during the spring and summer upwelling season in the Central California current upwelling regime. Cont. Shelf Res. **66**: 58–72. doi:10.1016/j.csr.2013.07.003

Biller, D. V., and K. W. Bruland. 2014. The Central California Current transition zone: A broad region exhibiting evidence for iron limitation. Prog. Oceanogr. **120**: 370–382. doi:10.1016/j.pocean.2013.11.002

Bruland, K. W., E. L. Rue, and G. J. Smith. 2001. Iron and macronutrients in California coastal upwelling regimes: Implications for diatom blooms. Limnol. Oceanogr. **46**: 1661–1674. doi:10.4319/lo.2001.46.7.1661

Bruland, K. W., E. L. Rue, G. J. Smith, and G. R. Ditullio. 2005. Iron, macronutrients and diatom blooms in the Peru upwelling regime: Brown and blue waters of Peru. Mar. Chem. **93**: 81–103. doi:10.1016/j.marchem.2004.06.011

Bruland, K. W., M. C. Lohan, A. M. Aguilar-Islas, G. J. Smith, B. Sohst, and A. Baptista. 2008. Factors influencing the chemistry of the near-field Columbia River plume: Nitrate, silicic acid, dissolved Fe, and dissolved Mn. J. Geophys. Res.: C00B02. doi:10.1029/2007JC004702

Bruland, K. W., R. Middag, and M. C. Lohan. 2014. Controls of trace metals in seawater, treatise on geochemistry, 2nd ed. Elsevier. doi:10.1016/B978-0-08-095975-7.00602-1.

Brzezinski, M. A., J. W. Krause, R. M. Bundy, K. A. Barbeau, P. Franks, R. Goericke, M. R. Landry, and M. R. Stukel. 2015. Enhanced silica ballasting from iron stress sustains carbon export in a frontal zone within the California Current. J. Geophys. Res. Oceans **120**: 4654–4669. doi:10.1002/2015JC010829

Carr, M. E. 2002. Estimation of potential productivity in Eastern Boundary Currents using remote sensing. Deep-Sea Res. Part II **49**: 59–80. doi:10.1016/S0967-0645(01)00094-7

Chappell, P. D., L. P. Whitney, J. R. Wallace, A. I. Darer, S. Jean-Charles, and B. D. Jenkins. 2015. Genetic indicators of iron limitation in wild populations of *Thalassiosira oceanica* from the northeast Pacific Ocean. ISME J. **9**: 592–602. doi:10.1038/ismej.2014.171

Chase, Z., P. G. Strutton, and B. Hales. 2007. Iron links river runoff and shelf width to phytoplankton biomass along the US west coast. Geophys. Res. Lett. **34**: LO4607. doi:10.1029/2006GL028069

Checkley, D. M., and J. A. Barth. 2009. Patterns and processes in the California Current System. Prog. Oceanogr. **83**: 49–64. doi:10.1016/j.pocean.2009.07.028

Cohen, N. R., and others. 2017. Diatom transcriptional and physiological responses to changes in iron bioavailability across ocean provinces. Front. Mar. Sci. **4**: 360. doi:10.3389/fmars.2017.00360

Cutter, G. A., P. Andersson, L. Codispoti, P. Croot, R. Francois, M. Lohan, H. Obata, and M. R. van der Loeff (2014), Sampling and sample-handling protocols for GEOTRACES cruises, version 2.0. Available from http://www.geotraces.org/images/stories/documents/intercalibration/Cookbook.pdf

Elrod, V. A., W. M. Berelson, K. H. Coale, and K. S. Johnson. 2004. The flux of iron from continental shelf sediments: A missing source for global budgets. Geophys. Res. Lett. **31**: L12307. doi:10.1029/2004GL020216

Firme, G. F., E. L. Rue, D. A. Weeks, K. W. Bruland, and D. A. Hutchins. 2003. Spatial and temporal variability in phytoplankton iron limitation along the California coast and consequences for Si, N, and C biogeochemistry. Global Biogeochem. Cycles **17**: 1016. doi:10.1029/2001GB001824

Gorbunov, M. Y., and P. G. Falkowski. 2005. Fluorescence induction and relaxation (FIRe) technique and instrumentation for monitoring photosynthetic processes and primary production in aquatic ecosystems, p. 1029–1031. In A. Van Der Est [eds.], Photosynthesis: Fundamental aspects to global perspectives. Allen Press.

Hutchins, D. A., and K. W. Bruland. 1998. Iron-limited diatom growth and Si:N uptake ratios in a coastal upwelling regime. Lett. Nat. **393**: 561–564. doi:10.1038/31203

Hutchins, D. A., G. R. Ditullio, Y. Zhang, and K. W. Bruland. 1998. An iron limitation mosaic in the California upwelling regime. Limnol. Oceanogr. **43**: 1037–1054. doi:10.4319/lo.1998.43.6.1037

Huyer, A. 1983. Coastal upwelling in the California Current System. Prog. Oceanogr. **12**: 259–284. doi:10.1016/0079-6611(83)90010-1

Johnson, K. S., F. P. Chavez, and G. E. Friederich. 1999. Continental-shelf sediment as a primary source of iron for coastal phytoplankton. Nature **398**: 697–700. doi:10.1038/19511

King, A. L., and K. Barbeau. 2007. Evidence for phytoplankton iron limitation in the southern California Current System. Mar. Ecol. Prog. Ser. **342**: 91–103. doi:10.3354/meps342091

Kolber, Z. S., O. Prášil, and P. G. Falkowski. 1998. Measurements of variable chlorophyll fluorescence using fast repetition rate techniques: Defining methodology and experimental protocols. BBA-Bioenergetics **1367**: 88–106. doi:10.1016/S0005-2728(98)00135-2

Kudela, R., N. Garfield, and K. Bruland. 2006. Bio-optical signatures and biogeochemistry from intense upwelling and relaxation in coastal California. Deep-Sea Res. Part II **53**: 999–3,022. doi:10.1016/j.dsr2.2006.07.010

Lohan, M. C., A. M. Aguilar-Islas, R. P. Franks, and K. W. Bruland. 2005. Determination of iron and copper in seawater at pH 1.7 with a new commercially available chelating resin, NTA Superflow. Anal. Chim. Acta **530**: 121–129. doi:10.1016/j.aca.2004.09.005

Lohan, M. C., A. M. Aguilar-Islas, and K. W. Bruland. 2006. Direct determination of iron in acidified (pH 1.7) seawater samples by flow injection analysis with catalytic spectrophotometric detection: Application and intercomparison. Limnol. Oceanogr.: Methods **4**: 164–171. doi:10.4319/lom.2006.4.164

Lohan, M. C., and K. W. Bruland. 2008. Elevated Fe(II) and dissolved Fe in hypoxic shelf waters off Oregon and Washington: And enhanced source of iron to coastal upwelling regimes. Environ. Sci.Technol. **42**: 6462–6468. doi:10.1021/es800144j

Love, M. I., W. Huber, and S. Anders. 2014. Moderated estimation of fold change and dispersion for RNA-seq data with DESeq2. Genome Biol. **15**: 550. doi:10.1186/s13059-014-0550-8

Lynn, R. J., and J. J. Simpson. 1987. The California Current System: The seasonal variability of its physical characteristics. J. Geophys. Res. **92**: 12947–12966. doi:10.1029/JC092iC12p12947

Marchetti, A., and M. T. Maldonado. 2016. Iron, p. 233–279. *In* M. A. Borowitzka, J. Beardell, and J. Raven [eds.], The physiology of microalgae. Springer Publishing.

Marchetti, A., C. M. Moreno, N. H. Cohen, I. Oleinikov, K. deLong, B. S. Twining, E. V. Armbrust, and R. H. Lampe. 2017. Development of a molecular-based index for assessing iron status in bloom-forming pennate diatoms. J. Phycol. **53**: 820–832. doi:10.1111/jpy.12539

Monod, J. 1942. Recherche sur la croissance des cultures bactériennes. Actualités scientifiques et industrielles. Annual Review of Microbiology **3**: 3–71.

Parsons, T. R., Y. Maita, and C. M. Lalli. 1984. A manual of chemical and biological methods for seawater analysis. Pergamon Press Ltd.

Redfield, A. C. 1958. The biological control of chemical factors in the environment. Am. Sci. **46**: 205–221.

Sarthou, G., K. R. Timmermans, S. Blain, and P. Treguer. 2005. Growth physiology and fate of diatoms in the ocean: A review. J. Sea Res. **53**: 25–42. doi:10.1016/j.seares.2004.01.007

Strub, P. T., J. S. Allen, A. Huyer, and R. L. Smith. 1987. Large-scale structure of the spring transition in the coastal ocean off western North America. J. Geophys. Res. **92**: 1527–1544. doi:10.1029/JC092iC02p01527

Sunda, W. G., and S. A. Huntsman. 1995. Iron uptake and growth limitation in oceanic and coastal phytoplankton. Mar. Chem. **50**: 189–206. doi:10.1016/0304-4203(95)00035-P

Wells, M. L. 1999. Manipulating iron availability in nearshore waters. Limnol. Oceanogr. **44**: 1002–1008. doi:10.4319/lo.1999.44.4.1002

Wheatcroft, R. A., C. K. Sommerfield, D. E. Drake, J. C. Borgeld, and C. A. Nittrouer. 1997. Rapid and widespread dispersal of flood sediment on the northern California margin. Geology **25**: 163–166. doi:10.1130/0091-7613(1997)025<0163:RAWDOF>2.3.CO;2

Xu, J. P., M. Noble, and S. L. Eittreim. 2002. Suspended sediment transport on the continental shelf near Davenport, California. Mar. Geol. **181**: 171–193. doi:10.1016/S0025-3227(01)00266-3

Zaba, K. D., and D. L. Rudnick. 2016. The 2014-2015 warming anomaly in the Southern California Current System observed by underwater gliders. Geophys. Res. Lett. **43**: 1241–1248. doi:10.1002/2015GL067550

Zentara, S.-J., and D. Kamykowski. 1977. Latitudinal relationships among temperature and selected plant nutrients along the west coast of North and South America. J. Mar. Res. **35**: 321–337.

Acknowledgments

The authors thank the captain and crew of the R/V *Melville*, Dondra Biller for her vast assistance with flow injection analysis, satellite imaging code, and for downloading satellite data while we were at sea, and Geoffrey Smith, Travis Mellett, and Matthew Brown for assistance with sample collection. Benjamin Twining, Jeremy Jacquot, and Kelsey Ellis assisted with the incubation experiments and Kim Thamatrakoln and Fedor Kuzminov provided FRRF measurements. This work was funded by the National Science Foundation through award numbers OCE 1259776 to K.W.B. and OCE 1334935 to A.M.

Conflict of Interest

None declared.

Submitted 13 December 2017
Revised 18 May 2018
Accepted 13 July 2018

Associate editor: James Moffett